



# Understanding the role of Keggin type heteropolyacid catalysts for glycerol acetylation using toluene as an entrainer

S.S. Kale<sup>a</sup>, U. Armbruster<sup>a</sup>, R. Eckelt<sup>a</sup>, U. Bentrup<sup>a</sup>, S.B. Umbarkar<sup>b</sup>, M.K. Dongare<sup>b,c</sup>, A. Martin<sup>a,\*</sup>

<sup>a</sup> Leibniz-Institut für Katalyse e. V. an der Universität Rostock, Albert-Einstein-Str. 29a, D-18059 Rostock, Germany

<sup>b</sup> Catalysis Division, CSIR-National Chemical Laboratory, Pune 411008, India

<sup>c</sup> Moj Engineering Systems Ltd., 15-81/B, MIDC, Bhosari, Pune 411026, India



## ARTICLE INFO

### Article history:

Received 27 April 2016

Received in revised form 28 July 2016

Accepted 17 August 2016

Available online 18 August 2016

### Keywords:

Glycerol

Acetylation

Azeotropes

Heteropolyacids

Triacetin

Heterogeneous catalyst

## ABSTRACT

The heterogeneously catalyzed esterification (acetylation) of glycerol toward triacetin in batch mode in presence of toluene as entrainer was studied. Silicotungstic acid, tungstophosphoric acid and phosphomolybdic acid as heteropolyacids (HPAs) supported on silica, alumina or silica-alumina were used as catalysts. The course of the reaction was found to be very sensitive to the nature of the HPA as well as the support. Solid characterization by Raman spectroscopy, XRD, and pyridine-FTIR revealed that only combinations of tungsten-based HPAs and silica support were able to preserve the structure of active component throughout the preparation process, which was essential to obtain active and selective catalysts. The interaction between HPA and support was decisive for stability and dispersion of the catalytically active species. With the best performing catalyst  $H_4SiW_{12}O_{40}/SiO_2$ , selectivity to triacetin reached 71% at complete conversion within 24 h. The high selectivity to triacetin is attributed the Brønsted acidic sites originated from stabilized Keggin structure and continuous removal of water during course of reaction. Toluene is able to form azeotropic mixtures with water and acetic acid and keeps the reaction temperature below the boiling point of acetic acid. Thus, water-free reaction conditions can be established. The catalyst was reusable; however, the activity and selectivity towards triacetin slightly decreased in a repetition run due to loss of active sites.

© 2016 Elsevier B.V. All rights reserved.

## 1. Introduction

Glycerol is inevitably produced in the biodiesel production from transesterification of vegetable oil or animal fats and has led to a drastic surplus in chemical market. Global production of biodiesel market is estimated to reach 36.9 million metric tons in 2020, which will give approximately 3.7 million metric tons of crude glycerol [1–3]. The current use of glycerol in pharmaceuticals, food and cosmetics consumes only a small part and hence, demand is somehow limited. To sustain chemical market and industry, it is important to convert glycerol into value added chemicals by several catalytic processes, such as selective oxidation to glyceric acid or hydroxy-acetone [4], dehydration to acrolein [5–7], hydrogenolysis to 1,2- or 1,3-propanediol [8], etherification to alkyl ether [9,10], condensation to dimers or higher oligomers [11] and many others [3,12]. Another interesting approach to convert glycerol into monoacetyl glycerol (MAG, monoacetin), diacetyl glycerol (DAG, diacetin) and

triacyl glycerol (TAG, triacetin) by means of esterification with acetic acid (acetylation) as shown in Fig. 1. These products have application in food and leather industry, as plasticizers and also they may serve as solvent and fuel additive [13–15].

Glycerol acetylation is an acid catalyzed reaction with equimolar formation of water as by-product at every consecutive step and the chemical equilibrium limits the extent of the esterification. In addition, Gibbs free energies of the first two acetylation steps (MAG and DAG) are 19.15 and 17.80 kJ/mol, respectively, whereas this value for the third step (TAG) is relatively high (55.58 kJ/mol) and thus, the third step should be the most difficult one [16]. Beyond that, elevated temperatures are necessary to obtain high reaction rates. Generally the reaction is performed using homogeneous catalysts like sulfuric acid and paratoluene sulfonic acid [17] or heterogeneous catalysts such as sulphated mesoporous silica [18], sulphated zirconia [19,20], sulphated activated carbon [21,22], double SO<sub>3</sub>H-functionalized ionic liquids [23] and acid ion exchange resins like Amberlyst-15 or Amberlyst-36 [24–26]. On the other side, use of acetic anhydride as acetylation agent instead of acetic acid boosts the selectivity to TAG close to 100% as no water is formed, and the reaction rates are high even in the absence of catalysts. However,

\* Corresponding author.

E-mail address: [andreas.martin@catalysis.de](mailto:andreas.martin@catalysis.de) (A. Martin).

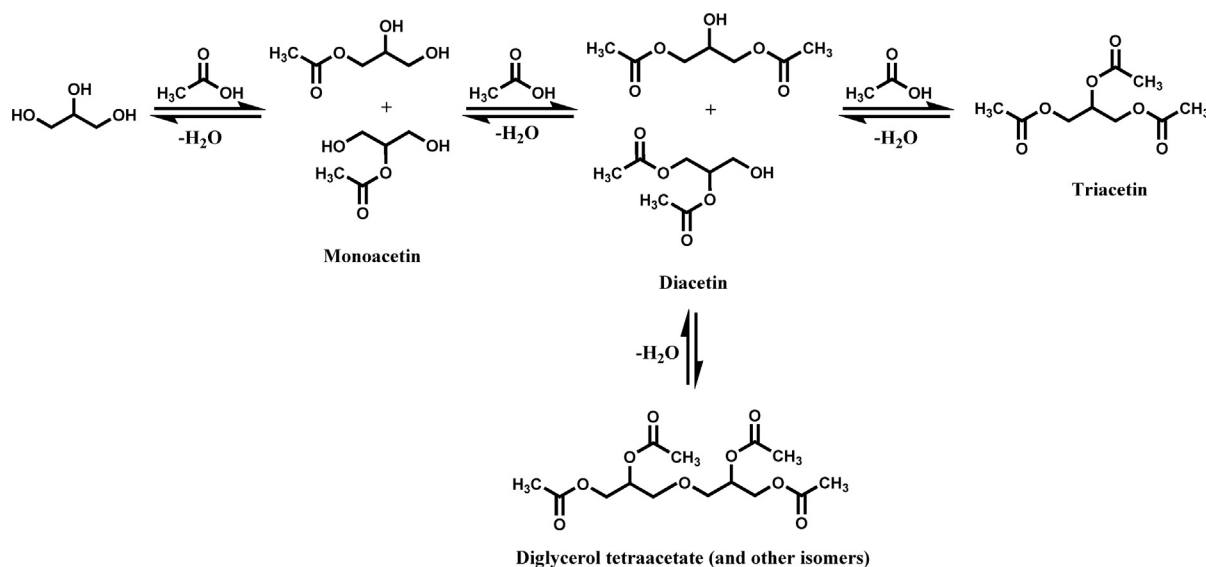


**Fig. 1.** Reaction scheme for consecutive glycerol acetylation.

acetic anhydride is more expensive and hazardous than acetic acid, and it is not environmentally friendly [27,28].

Furthermore, supported heteropolyacids have been employed for glycerol acetylation reaction. Phosphomolybdic acid engaged in a zeolite catalyst showed 68% glycerol conversion with only 2% selectivity to TAG [29]. Very recently, Patel et al. used MCM-41 and ZrO<sub>2</sub> supported tungstophosphoric acid catalysts but the selectivity to TAG was found to be rather low with 15% and 4%, respectively [30]. The same group also used 30 wt% tungstophosphoric acid impregnated on MCM-48 as catalyst with 30% selectivity to TAG using an acetic acid/glycerol molar ratio of 6 [31]. Silicotungstic acid supported on zirconia showed 32.3% selectivity to TAG with complete conversion of glycerol using acetic acid/glycerol molar ratio of 10 [32]. Huang et al. used tungstophosphoric acid immobilized on ionic liquid as a homogeneous catalyst which showed 98% selectivity to TAG using a high acetic acid/glycerol molar ratio of 10 and toluene as an entrainer under nitrogen flow of 150 ml/h [33].

In general, glycerol acetylation with acetic acid strongly depends on the acidic properties of the catalysts, but it is equilibrium controlled due to formation of water. A recent study from our group has shown that the use of toluene as an entrainer allows to remove formed water immediately by azeotropic distillation and to shift the equilibrium almost completely towards TAG using ion exchange resins Amberlyst-15 or Amberlyst-70 as catalysts [34].

The aim of this present work is to evaluate the catalytic activity of different HPA supported on oxides with large surface area under such water-free conditions with respect to catalyst structure and amount of acid sites. Silica, alumina and silica-alumina supported HPA (STA, TPA and PMA) catalysts were synthesized, characterized in fresh and spent state and evaluated in glycerol acetylation reaction. The results were compared with reference experiments either without catalyst (blank tests) or homogeneously catalyzed (pure HPAs are dissolved in acetic acid) under same reaction conditions and correlated with physiochemical properties of the catalysts.

## 2. Experimental

### 2.1. Materials

The organic compounds glycerol (Alfa Aesar, Germany, >99%), acetic acid (Fisher chemicals, Analytical reagent grade), toluene (Acros Organics, analytical reagent grade) and the silico-

tungstic acid (STA, Fluka), tungstophosphoric acid (TPA, Fluka), phosphomolybdic acid (PMA, Merck) and the supports silica-alumina (SIRAL® 40; SiO<sub>2</sub>/Al<sub>2</sub>O<sub>3</sub> = 40: 60), dispersible alumina (Disperal®/SASOL) as precursor for γ-alumina (γ-Al<sub>2</sub>O<sub>3</sub>) and silica (SS61138 Chempur/SiO<sub>2</sub>) were used as received. Furthermore, trimethylchlorosilane and hexamethyl disilazane (Aldrich), dodecane (TCI Europe), hexadecane (Aldrich) and pyridine (ACROS) were used for analytical purposes.

### 2.2. Catalyst preparation

While the silica and silica-alumina supports were not treated before use, dispersible alumina Disperal P2® was used as a precursor to prepare mesoporous γ-Al<sub>2</sub>O<sub>3</sub> with tailor-made properties. In a typical procedure, 70 g Disperal P2® was added to 350 g distilled water and stirred for 1 h; to this solution, 78 g Triton X-100 template and 30 g aqueous ammonium acetate solution (33 wt%) were added to form a white gel. This gel was further dried in air at 110 °C and calcined in air at 600 °C for 4 h. The other supports SiO<sub>2</sub> and SiO<sub>2</sub>-Al<sub>2</sub>O<sub>3</sub> were calcined in air at 500 °C for 5 h before impregnation.

The heteropolyacids STA, TPA, and PMA were supported onto the three supports by wet impregnation method with a nominal HPA loading of 20 wt%. In the typical procedure for STA/SiO<sub>2</sub>, an aqueous solution (10 ml) of STA (2 g) and some rinsing water (8 ml) was added to the silica (8 g) under constant stirring overnight. In total 18 ml of water was used for synthesis. Excess water was removed using a rotary evaporator. The obtained solid was dried at 120 °C for 2 h and then calcined at 300 °C with air in a muffle for 4 h to obtain the powdery catalyst.

### 2.3. Characterization of catalysts

BET surface area, pore volume and pore diameter of the catalysts were determined from the nitrogen adsorption/desorption isotherms at –196 °C on a Micromeritics ASAP 2010 instrument. Before the measurement, each sample was evacuated at 200 °C for 4 h. The average pore diameters were calculated according to the BJH method.

Powder X-ray diffraction (XRD) patterns were measured on a theta/theta diffractometer (X'Pert Pro from Panalytical, Almelo, Netherlands) with CuKα radiation ( $\lambda = 0.015418 \text{ nm}$ , 40 kV, 40 mA) and an X'Celerator RTMS detector. The alignment was checked by

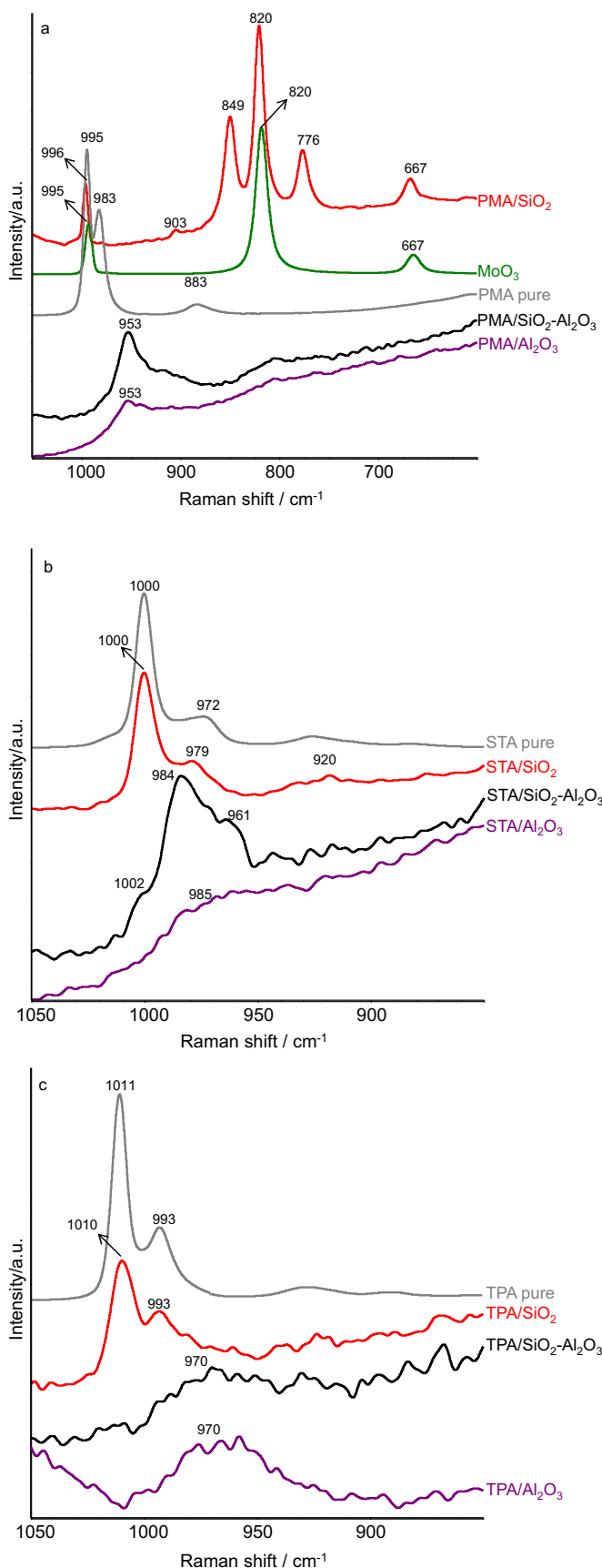


**Fig. 2.** Raman spectra of a) STA/SiO<sub>2</sub>, STA/SiO<sub>2</sub>-Al<sub>2</sub>O<sub>3</sub> and STA/Al<sub>2</sub>O<sub>3</sub> and, b) TPA/SiO<sub>2</sub>, TPA/SiO<sub>2</sub>-Al<sub>2</sub>O<sub>3</sub> and TPA/Al<sub>2</sub>O<sub>3</sub> and c) PMA/SiO<sub>2</sub>, PMA/SiO<sub>2</sub>-Al<sub>2</sub>O<sub>3</sub>, PMA/Al<sub>2</sub>O<sub>3</sub> and reference materials (bulk HPA and MoO<sub>3</sub>).

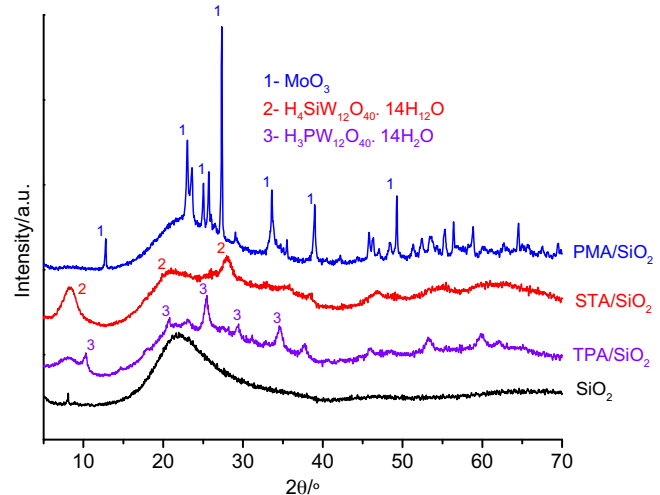


**Fig. 3.** X-Ray diffractograms of used SiO<sub>2</sub>, TPA/SiO<sub>2</sub>, STA/SiO<sub>2</sub> and PMA/SiO<sub>2</sub>.

means of silicon standard. The data were collected in the 2 theta range from 5–70°. The phase composition of the samples was determined using the program suite WinXPOW by STOE&CIE with inclusion of the Powder Diffraction File (PDF) data base of the ICDD (International Centre of Diffraction Data).

The Raman spectra were recorded using a fiber optical RXN-Spectrometer (Kaiser Optical System) equipped with a 10–400 mW diode laser for excitation at a wavelength of 785 nm and a Mk II Filtered Probe Head with a non-contact optics. The measurements were performed with 70 mW. The spectra were recorded with 3 accumulations and 3 s exposure time.

For surface acidity measurement by means of IR spectroscopy pyridine was used as probe molecule. The measurements in transmission mode were carried out on a Bruker Tensor 27 spectrometer equipped with a heatable homemade reaction cell with CaF<sub>2</sub> windows connected to a gas-dosing and evacuation system. The sample powders were pressed into self-supporting wafers with a diameter of 20 mm and a weight of 50 mg. Before pyridine adsorption, the samples were pretreated by heating in synthetic air to 300 °C for 10 min, subsequent cooling to room temperature and evacuation. Pyridine was adsorbed at room temperature by means of a carrier gas passing through a saturator filled with pyridine until saturation of sample surface. Then the reaction cell was evacuated to remove physisorbed pyridine. The desorption of pyridine chemisorbed on acid sites was followed by heating the sample in vacuum to 300 °C and recording spectra every 50 °C.

For the determination of the composition by means of ICP-OES technique, a Varian 715-ES ICP-Emission-Spectrometer was used. Approximately 20 mg of the sample was mixed with 8 ml of aqua regia and 2 ml of hydrofluoric acid. The digestion was performed in a microwave-assisted sample preparation system “MULTIWAVE” from Anton Paar/Perkin-Elmer at ~200 °C and ~65 bar pressure. The digested solution was filled up to 100 ml and analyzed. The data analysis was performed on the Varian 715-ES software “ICP Expert”.

Tungsten leached into the reaction mixture was analyzed qualitatively by XRF performed on a BRUKER S2 RANGER instrument.

#### 2.4. Catalyst tests

Glycerol acetylation was performed in a three-necked 250 ml glass flask equipped with a fractionating Vigreux column, a modified Dean-Stark apparatus equipped with thermometer to measure the temperature of the boiling azeotropic mixture and a reflux condenser as described in detail elsewhere [34]. The flask was also

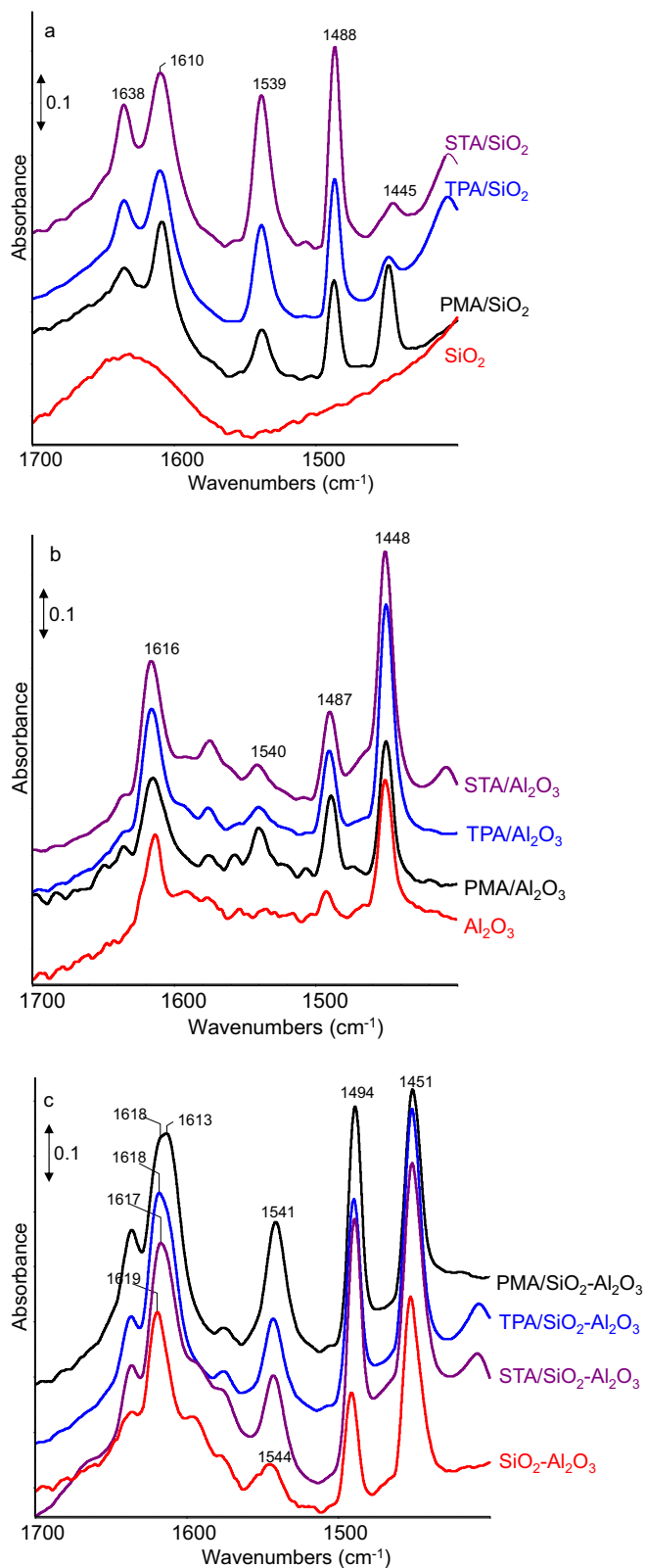


**Fig. 4.** FTIR spectra of adsorbed pyridine on a)  $\text{SiO}_2$ , TPA/ $\text{SiO}_2$ , STA/ $\text{SiO}_2$  and PMA/ $\text{SiO}_2$  b)  $\text{Al}_2\text{O}_3$ , TPA/ $\text{Al}_2\text{O}_3$ , STA/ $\text{Al}_2\text{O}_3$  and PMA/ $\text{Al}_2\text{O}_3$  and c)  $\text{SiO}_2\text{-Al}_2\text{O}_3$ , TPA/ $\text{SiO}_2\text{-Al}_2\text{O}_3$ , STA/ $\text{SiO}_2\text{-Al}_2\text{O}_3$ , PMA/ $\text{SiO}_2\text{-Al}_2\text{O}_3$  at 150 °C.

equipped with a glass tube (with thermocouple) to monitor directly the temperature of the reaction mixture. The reaction mixture was heated using an oil bath (oil bath temperature 150 °C; reaction mixture temperature 105 °C) and both reaction mixture and oil bath were stirred using a magnetic stirrer (1200 rpm) for intensive mixing and to improve heat transfer. Typically the flask was charged with 10 g glycerol (0.108 mol) and 39.16 g acetic acid (0.652 mol), representing an acetic acid to glycerol ratio of 6: 1, 60 g toluene (0.652 mol) and 1 g dodecane (internal standard to evaluate liquid volume change). After heating the reaction mixture to desired temperature, 500 mg catalyst was added. This was defined as starting time of the reaction. During the running test, samples of 100  $\mu\text{l}$  volume were withdrawn periodically. Besides the regular catalyst tests, homogeneous reaction with dissolved STA, TPA and PMA as well as a blank test in absence of any catalyst were carried out under similar reaction conditions. The total catalyst weight used in the latter reactions with pure HPA (0.1 g) was equal to the HPA load (20 wt%) in the supported catalysts to allow comparison of the results.

With some catalysts, reusability experiments and stop experiments were conducted by removing catalyst from a regular experiment after a defined reaction time, addition of fresh glycerol-acetic acid feed and continuation of the run under identical reaction conditions as before. Such experiments also served as a cross-check of HPA leaching into the bulk liquid and any contribution of homogeneous catalysis.

## 2.5. Analytical procedures

For proper quantification of the highly polar compounds, the OH groups of unconverted glycerol, MAG and DAG were silylated before gas chromatographic analysis. In the typical procedure, 100  $\mu\text{l}$  of product samples were silylated using hexamethyl disilazane and trimethylchlorosilane with pyridine as solvent. In addition, hexadecane was always used as an internal standard for the GC analysis (this means that two internal standards were used to cover the complete analysis procedure). Thereby prepared product samples in close vial were kept at 70 °C in a drying oven for 45 min and then analyzed using a gas chromatograph (HP 5890 series II) equipped with a CP-Sil 13 CB column (25 m × 0.32 mm) and FID detector. The temperature program was as follows: 50 °C for 1 min hold, heating at 20 K/min to 310 °C, 2 min hold at 310 °C. The educts glycerol and acetic acid as well as the silylated products MAG, DAG and TAG were clearly eluted. Peak assignment and calibration of GC detector were carried out by means of authentic compounds that were prepared at high purity by fractionated distillation. For DAG, two isomers were detected in the chromatograms, but separation was incomplete and individual quantification was impossible. The relative error of this analytical procedure was below 1%. All reported conversion data refer to glycerol.

## 3. Results and discussion

### 3.1. Catalyst characterization

#### 3.1.1. Textural properties

**Table 1** represents the BET surface areas, pore volumes and average pore diameters for the supported HPA catalysts prepared with 20 wt% loading in addition to bare supports. The data indicate a remarkable decrease in the BET surface area (by 6–35%) as well as in the pore volume after impregnation due to the blockage of pores of the support with the HPA components; however, this is no surprise when regarding the high HPA loading of 20 wt%. The pore diameters range from 7.8–12.0 nm which is typical for mesoporous material. Interestingly, only a marginal decrease in the average pore diam-

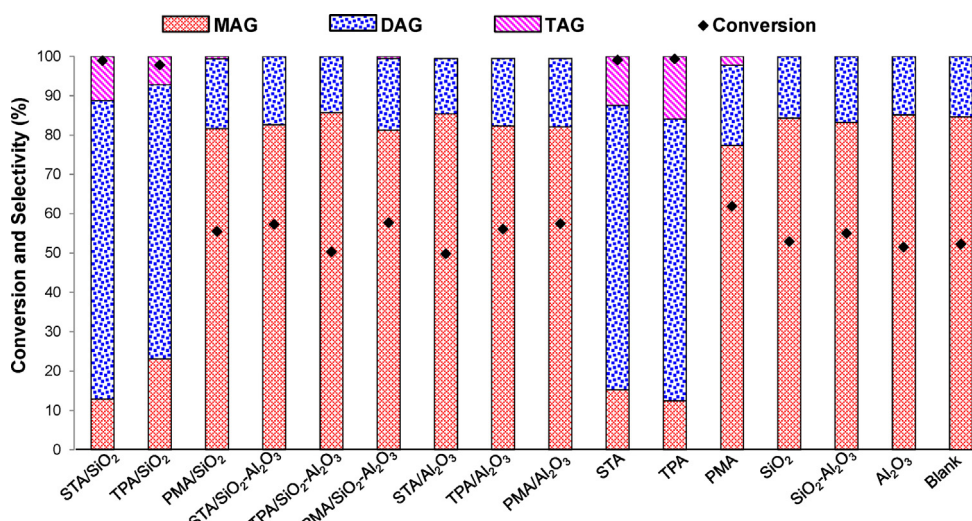


**Fig. 5.** Glycerol esterification with acetic acid and toluene as an entrainer (glycerol = 10 g, acetic acid = 39.16 g, molar ratio acetic acid: glycerol = 6: 1, toluene = 60 g, 105 °C, 4 h; catalyst mass = 0.5 g (supported) or 0.1 g (bulk HPA)).

**Table 1**  
Textural properties of supports and catalysts.

Catalyst	$A_{\text{BET}}$ ( $\text{m}^2/\text{g}$ )	Deviation relative to support (%)	Pore volume ( $\text{cm}^3/\text{g}$ )	Average pore diameter (nm)
SiO <sub>2</sub>	244	–	0.84	12.0
STA/SiO <sub>2</sub>	206	-15.6	0.66	11.9
TPA/SiO <sub>2</sub>	206	-15.6	0.62	11.7
PMA/SiO <sub>2</sub>	229	-6.1	0.76	11.9
Al <sub>2</sub> O <sub>3</sub>	303	–	1.32	11.4
STA/Al <sub>2</sub> O <sub>3</sub>	228	-24.7	0.68	12.1
TPA/Al <sub>2</sub> O <sub>3</sub>	267	-11.9	0.84	11.8
PMA/Al <sub>2</sub> O <sub>3</sub>	228	-24.7	0.79	11.8
SiO <sub>2</sub> -Al <sub>2</sub> O <sub>3</sub>	520	–	1.00	8.4
STA/SiO <sub>2</sub> -Al <sub>2</sub> O <sub>3</sub>	350	-32.7	0.73	8.4
TPA/SiO <sub>2</sub> -Al <sub>2</sub> O <sub>3</sub>	341	-34.4	0.67	7.4
PMA/SiO <sub>2</sub> -Al <sub>2</sub> O <sub>3</sub>	377	-27.5	0.81	7.8

eter was observed after impregnation, and the data for catalysts with the same support are almost the same.

### 3.1.2. Raman spectroscopy

Raman spectroscopy is a well-known technique to investigate Keggin structures of HPAs on the surface of a support. Raman spectra of all fresh supported catalysts and additionally of pure bulk STA, TPA, PMA and also MoO<sub>3</sub> were recorded and compared as shown in Fig. 2.

Pure bulk PMA shows Raman bands at 996  $\text{cm}^{-1}$  and 983  $\text{cm}^{-1}$ , which can be assigned to the stretching vibration of terminal Mo=O, and additionally a less intense band appears at 883  $\text{cm}^{-1}$  for bending vibration for Mo—O—Mo units [35,36] (Fig. 2a). The spectrum of PMA/SiO<sub>2</sub> reveals bands at 995  $\text{cm}^{-1}$  (low intensity), 903  $\text{cm}^{-1}$  (very low intensity), 849  $\text{cm}^{-1}$  (moderate intensity), 820  $\text{cm}^{-1}$  (high intensity, main band), 776  $\text{cm}^{-1}$  (moderate intensity) and 667  $\text{cm}^{-1}$  (low intensity). Comparing the spectrum of PMA/SiO<sub>2</sub> with the bulk MoO<sub>3</sub> spectrum, the bands at 820 and 667  $\text{cm}^{-1}$  might be assigned to orthorhombic  $\alpha$ -MoO<sub>3</sub> species formed by decomposition of the Keggin structure PMA. This has been reported also by other authors [37]. PMA/SiO<sub>2</sub> shows additional bands at 903, 849 and 776  $\text{cm}^{-1}$  which can be assigned to monoclinic  $\beta$ -MoO<sub>3</sub> surface species [38]. The spectra of PMA/SiO<sub>2</sub>-Al<sub>2</sub>O<sub>3</sub> and PMA/Al<sub>2</sub>O<sub>3</sub> show a broad band at 984  $\text{cm}^{-1}$ , indicating a high dispersion of PMA on the surface.

The Raman spectrum of bulk STA reveals an intense band at 1000  $\text{cm}^{-1}$ , a shoulder at 973  $\text{cm}^{-1}$  (stretching vibration of W=O)

and a weak band at 920  $\text{cm}^{-1}$  for the bending vibration of W—O—W (Fig. 2b). Comparing the spectrum of supported STA/SiO<sub>2</sub> with bulk STA, preservation of the bands at 1000  $\text{cm}^{-1}$  and 979  $\text{cm}^{-1}$  can be recognized. This clearly indicates that the Keggin structure  $[\text{SiW}_{12}\text{O}_{40}]^{4-}$  of STA is preserved on the surface of SiO<sub>2</sub>. The spectrum of STA/SiO<sub>2</sub>-Al<sub>2</sub>O<sub>3</sub> shows a broad band at 984  $\text{cm}^{-1}$  with additional shoulders at 1002 and 961  $\text{cm}^{-1}$ . This broad band might stem from partially deteriorated lacunary species  $[\text{SiW}_{11}\text{O}_{39}]^{8-}$  [39], formed by interaction of STA with surface acid sites.

Similar to STA, the Raman spectrum of bulk TPA exhibits the intense bands at 1011 and 993  $\text{cm}^{-1}$  for stretching vibrations of W=O and the band at 928  $\text{cm}^{-1}$  for bending vibration of W—O—W (Fig. 2c). The spectrum of TPA/SiO<sub>2</sub> also reveals bands at 1010, 993 and 925  $\text{cm}^{-1}$  indicating that the primary structure of TPA (Keggin  $[\text{PW}_{12}\text{O}_{40}]^{3-}$ ) is retained on the surface of SiO<sub>2</sub>. The spectrum of TPA/SiO<sub>2</sub>-Al<sub>2</sub>O<sub>3</sub> shows a broad band at 970  $\text{cm}^{-1}$  indicating the formation of either lacunary species  $[\text{PW}_{11}\text{O}_{39}]^{7-}$  or points to well dispersed Keggin species. [40]. The Raman spectrum of TPA/Al<sub>2</sub>O<sub>3</sub> exhibits similar structure as TPA/SiO<sub>2</sub>-Al<sub>2</sub>O<sub>3</sub>, represented by a broad band at 970  $\text{cm}^{-1}$ , most possibly due to interaction of Keggin TPA with Al<sub>2</sub>O<sub>3</sub> support.

The presented Raman results reveal that STA put on any support seems to be the most stable Keggin structure among the selected supports. Regarding the effect of nature of the support on HPA stability, a ranking in the order SiO<sub>2</sub>>SiO<sub>2</sub>-Al<sub>2</sub>O<sub>3</sub>>Al<sub>2</sub>O<sub>3</sub> can be established.

### 3.1.3. XRD

The XRD patterns of bare  $\text{SiO}_2$  and  $\text{SiO}_2$  supported HPA catalysts are depicted in Fig. 3. The bare  $\text{SiO}_2$  shows a broad reflection at  $24^\circ$  being typical for amorphous silica, which is also present in the supported samples (PDF 00-029-0085). STA/ $\text{SiO}_2$  indicates weak and broad (halo) reflections at  $8^\circ$ ,  $22^\circ$  and  $27^\circ$ , which might point to the high dispersion of STA over the surface of  $\text{SiO}_2$ . Similarly, the pattern for TPA/ $\text{SiO}_2$  indicates a low crystallinity due to high dispersion of the HPA. The related pattern reveals reflections at  $10^\circ$ ,  $27^\circ$ , and  $35^\circ$  that can be assigned to the Keggin structure of  $\text{H}_3\text{PW}_{12}\text{O}_{40} \cdot 6\text{H}_2\text{O}$  (PDF 00-050-0304). In contrast to the first two samples, PMA/ $\text{SiO}_2$  shows sharp peaks at  $13^\circ$ ,  $23^\circ$ ,  $25^\circ$  and  $27^\circ$ , indicating the presence of  $\text{MoO}_3$  molybdate phase (PDF 00-089-7112). The  $\text{MoO}_3$  species most likely were formed by decomposition of heteropoly anions at elevated temperature. By the way, here we have a nice conformity with Raman information on  $\text{MoO}_3$  formation (cf. Fig. 2a). From the XRD analysis of STA/ $\text{SiO}_2$  and TPA/ $\text{SiO}_2$  samples, it can be concluded that heteropoly anions are preserved at least partly, but at high dispersion, and thus this technique is near to detection limit to identify the crystalline domains of respective Keggin structures. Both the  $\gamma$ -alumina and silica-alumina supported catalysts exhibit only broad support reflections, therefore, the XRD patterns are not shown here. None of the reflections can be assigned to the expected HPA structures.

### 3.1.4. FTIR spectra of adsorbed pyridine

The acidic properties of bare supports and the STA, TPA and PMA containing catalysts using  $\text{SiO}_2$ ,  $\text{SiO}_2\text{-Al}_2\text{O}_3$  and  $\text{Al}_2\text{O}_3$  as supports were investigated by recording the FTIR spectra of adsorbed pyridine, as shown in Fig. 4. Generally, pyridine is coordinatively adsorbed on Lewis acid sites (L-Py, LS) showing bands at  $1445\text{--}1460\text{ cm}^{-1}$  and  $1610\text{--}1620\text{ cm}^{-1}$ , while Brønsted acid sites ( $\text{PyH}^+$ , BS) are characterized by bands at  $1540\text{--}1548\text{ cm}^{-1}$  and  $1635\text{--}1640\text{ cm}^{-1}$  [41,42]. The typical bands at  $1445\text{--}1460\text{ cm}^{-1}$  for LS (L-Py) and  $1540\text{--}1548\text{ cm}^{-1}$  for BS ( $\text{PyH}^+$ ) were used to calculate the acid site concentration from the band intensities and the absorption coefficients given in [43].

Table 2 represents the acidic properties in terms of band intensities and concentration of BS and LS. The bare silica support did not contribute to any surface acidity. As expected from Raman results, STA and TPA supported on silica showed higher BS concentration than Lewis acidity, as the Keggin structures seem to be preserved. It also has to be pointed out that STA possesses one proton more than the other HPAs. On the other side, PMA/ $\text{SiO}_2$  shows lower BS than LS concentration (Fig. 4a) as thermal decomposition of PMA into  $\text{MoO}_3$  species was observed in XRD and Raman spectroscopic studies. It is evident that the Brønsted acidity of the catalysts on this support correlates well with the stability of the HPAs in the order STA > TPA > PMA.

In contrast to the pure  $\text{SiO}_2$  support, the acid site concentration of bare  $\text{Al}_2\text{O}_3$  support reveals very strong Lewis acidity without any Brønsted acidity (Fig. 4b). The samples STA/ $\text{Al}_2\text{O}_3$  and TPA/ $\text{Al}_2\text{O}_3$  show less Brønsted acidity than PMA/ $\text{Al}_2\text{O}_3$  might be due to stronger interaction with the support. On the other hand, PMA/ $\text{Al}_2\text{O}_3$  exhibits strong Brønsted acidity compared to STA/ $\text{Al}_2\text{O}_3$  and TPA/ $\text{Al}_2\text{O}_3$  catalysts, most likely due to formed  $\text{MoO}_3$  species which show Brønsted acidic sites.

Interestingly, the acid site concentration of bare silica-alumina support reveals high Lewis acidity and a moderate contribution from BS (Fig. 4c). Surprisingly, the  $\text{SiO}_2\text{-Al}_2\text{O}_3$  supported HPAs showed the opposite trend in the concentration of BS as compared to  $\text{SiO}_2$  supported samples: STA < TPA < PMA. At the same time, the concentration of LS stays rather unaffected. This indicates that none of the tungsten containing HPAs seems to decompose with simultaneous formation of new LS as observed for the silica supported samples. A possible explanation for the observed trend in Brønsted

acidity might be that this  $\text{SiO}_2\text{-Al}_2\text{O}_3$  support offers plenty of reactive sites and a considerable amount of BS from HPA might interact with those via dehydration or condensation during calcination. It is also known that LS can be transformed into BS in the presence of water at elevated temperatures [44].

### 3.2. Catalytic test runs

Glycerol acetylation is a consecutive reaction with stepwise formation of MAG, DAG and TAG together with their respective isomers along with water as an unavoidable side-product. In the presence of water, each reaction step is controlled by chemical equilibrium. The equilibrium can be shifted towards the products by adding acetic acid in excess (to operate at high glycerol conversion) or by removing one of the products (preferably water) permanently during the reaction, e.g. by means of azeotropic distillation using an entrainer like toluene. In a recent study with ion exchange resins as catalysts at such reaction conditions, we could maintain a very low stationary water concentration of 0.05% which was shown to have a significant positive impact on reaction rates, selectivities and catalyst stability [34]. We reported that without removal of water during reaction under identical conditions, the selectivity to triacetin was significantly low.

Originally, the reaction mixture was biphasic due to the limited miscibility of polar reactants in toluene, but starts to boil at  $100^\circ\text{C}$ , and conversion of glycerol to MAG takes place and at the same time the reaction mixture becomes homogeneous. As the reaction proceeds, the temperature in the reaction mixture and on the top of the modified Dean Stark apparatus increased. The temperature inside the flask remained at  $105^\circ\text{C}$  for a long time and finally reached  $110^\circ\text{C}$  (boiling point of toluene) after desired product (TAG) was formed in high quantity. Toluene is able to form an azeotropic mixture with water at  $84^\circ\text{C}$  as well as with acetic acid at  $104^\circ\text{C}$  [45], and hence, depending on the composition of the reaction mixture, two azeotropic mixtures may form during glycerol acetylation reaction. This explains the observed course of the reaction temperature.

For comparison, the reaction was initially performed in the absence of catalyst (blank test; molar ratio of acetic acid: glycerol = 6, temperature =  $105^\circ\text{C}$ , 4 h). The glycerol conversion reached 52% after 4 h and the selectivities for MAG and DAG were 85% and 15%, respectively, without formation of TAG. The course of glycerol conversion and product selectivities is given in Table 3, which follows the well-known behavior of a consecutive reaction.

Fig. 5 gives an overview of glycerol acetylation using supported STA, TPA and PMA catalysts, bare supports  $\text{SiO}_2$ ,  $\text{SiO}_2\text{-Al}_2\text{O}_3$  and  $\text{Al}_2\text{O}_3$  and bulk STA, TPA and PMA solids. The results of the catalytic runs after 4 h of reaction time can be clearly separated into two groups according to the nature of the solids. The catalysts STA/ $\text{SiO}_2$  and TPA/ $\text{SiO}_2$  gave almost 100% glycerol conversion with a maximum selectivity of 70 and 75% to DAG and 11% and 7% selectivity to TAG, respectively. Surprisingly, the results obtained with the corresponding bulk STA and TPA solids showed almost similar results despite their much lower specific BET surface area, with almost 100% glycerol conversion after 4 h and selectivity to TAG of 12.4% and 16%, respectively. On the other hand, all catalysts using either  $\text{SiO}_2\text{-Al}_2\text{O}_3$  or  $\text{Al}_2\text{O}_3$  as support or PMA as active compound showed poor performance compared to tungsten-containing materials. In the related runs, the glycerol conversion never exceeded 65% and the product selectivities (MAG: 80–85%, DAG: 12–18%, TAG: < 3%) were comparable to the reaction without catalyst or with bare supports  $\text{SiO}_2$ ,  $\text{SiO}_2\text{-Al}_2\text{O}_3$  or  $\text{Al}_2\text{O}_3$  (Fig. 5).

It is known that bulk TPA and STA are more stable than PMA and these HPAs also follow the same order of their acid strength [46], which might explain the observed high activity of tungsten containing bulk HPAs. Although TPA has higher acid strength, the activity of  $\text{SiO}_2$  supported STA was found to be slightly higher, which can

**Table 2**

Acidic properties of pure carriers and supported heteropolyacids.

Catalyst	Intensity (150 °C) PyH <sup>+</sup> (1545 cm <sup>-1</sup> )	Brønsted acidity (μmol/g)	Intensity (150 °C) L-Py (1545 cm <sup>-1</sup> )	Lewis acidity (μmol/g)
SiO <sub>2</sub>	0	0	0	0
STA/SiO <sub>2</sub>	3.7	274.5	0.4	24.3
TPA/SiO <sub>2</sub>	2.1	154.9	0.6	31.1
PMA/SiO <sub>2</sub>	1.1	82.0	1.9	105.8
Al <sub>2</sub> O <sub>3</sub>	0	0	3.0	171.5
STA/Al <sub>2</sub> O <sub>3</sub>	0.5	40.6	5.0	280.7
TPA/Al <sub>2</sub> O <sub>3</sub>	0.5	38.4	5.3	297.7
PMA/Al <sub>2</sub> O <sub>3</sub>	0.9	65.4	3.0	168.7
SiO <sub>2</sub> –Al <sub>2</sub> O <sub>3</sub>	1.1	82.0	4.2	237.2
STA/SiO <sub>2</sub> –Al <sub>2</sub> O <sub>3</sub>	1.9	145.9	4.9	278.5
TPA/SiO <sub>2</sub> –Al <sub>2</sub> O <sub>3</sub>	2.0	150.4	5.1	289.8
PMA/SiO <sub>2</sub> –Al <sub>2</sub> O <sub>3</sub>	3.0	222.6	4.1	231.5

**Table 3**

Glycerol conversion and acetins formation in blank test run.

Time (h)	Glycerol conversion (%)	Selectivity to MAG (%)	Selectivity to DAG (%)	Selectivity to TAG (%)
1	28	99	1	0
2	31	92	8	0
3	44	88	12	0
4	52	85	15	0

(glycerol = 10 g, acetic acid = 39.16 g, molar ratio acetic acid: glycerol = 6, toluene = 60 g, 105 °C, time = 4 h).

be explained by the hydrolytic stability of STA (more resistant to water) and the higher total number of protons [46,47]. In the case of PMA, the obtained conversion was not higher than in the blank test, this may be due to the lower acid strength and thermal stability [48].

The high catalytic activity of STA/SiO<sub>2</sub> and TPA/SiO<sub>2</sub> compared to all other supported HPA catalysts used in the present study can be correlated first of all to the high Brønsted acidity (see Table 2) with simultaneous retention of HPA structure on silica support as seen in FTIR, XRD and Raman analyses. SiO<sub>2</sub>–Al<sub>2</sub>O<sub>3</sub> supported HPAs showed high Brønsted as well as Lewis acidity, whereas Al<sub>2</sub>O<sub>3</sub> supported catalysts revealed high Lewis acidity with very low Brønsted acidity and silica supported catalysts (except PMA/SiO<sub>2</sub>) showed high Brønsted acidity with very low Lewis acidity. In the latter case, the limited stability of PMA is the decisive factor and makes it a poor catalyst for acetylation reaction. The two best performing heterogeneous catalysts STA/SiO<sub>2</sub> and TPA/SiO<sub>2</sub> have by far the lowest number of Lewis sites. A high Lewis acidity does in no case allow high conversion even when the number of Brønsted sites is high (as found in STA/SiO<sub>2</sub>–Al<sub>2</sub>O<sub>3</sub>). It can be clearly stated that if one of these features (Brønsted acidity, structural integrity of HPA, low Lewis acidity) is changed, neither active nor selective catalyst is obtained.

On the other side, it is somewhat surprising that the much higher specific BET surface area as measured for supported catalysts has no measurable effect on conversion (and product distribution) as compared to parent bulk HPAs. This clearly indicates that activity and selectivity (product formation) seems to strongly depend on acid strength of the catalysts. To elucidate the leaching of active components from the tungsten-containing catalysts contributing to the possible homogeneous catalyzed reaction, separate experiments were carried out and discussed below.

### 3.3. Reaction progress monitoring

STA/SiO<sub>2</sub> and TPA/SiO<sub>2</sub> (besides the corresponding bulk HPA) showed highest catalytic activity compared to all other supported catalysts and supports. Hence, the performance of these catalysts was monitored over elongated run times (up to 24 h) to study the change in product selectivity toward TAG under the same reaction

conditions as described above (Fig. 6a and b). As expected for a consecutive product formation, with longer run time an increase in TAG selectivity was observed at the cost of MAG and DAG presence.

The product composition follows consequently the behavior of a consecutive reaction. Glycerol conversion reached more than 95% within the first 2 h of reaction time. The maximum selectivities of 36% and 48% for MAG were obtained with both catalysts within 1 h. The slightly better catalytic performance of STA/SiO<sub>2</sub> compared to TPA/SiO<sub>2</sub> is evident from the time to reach the maximum selectivity to DAG (STA/SiO<sub>2</sub>: 75% after 4 h; TPA/SiO<sub>2</sub>: 71% after 6 h). After 24 h, the selectivity to TAG was 71% with STA/SiO<sub>2</sub> and 67% with TPA/SiO<sub>2</sub>.

As the reaction proceeds, the by-product diglycerol tetraacetate (DGTA) was detected. We have reported the formation of DGTA already in studies with ion exchange resins as catalysts [34]. The formation of this by-product seems to be a special feature of glycerol acetylation under water-free conditions and high conversion. The DGTA selectivity after 24 h was 11.9% and 11.1% with STA/SiO<sub>2</sub> and TPA/SiO<sub>2</sub>, respectively. DGTA is expected to form most likely by oligomerization of MAG and/or DAG as we never observed diglycerol (oligomerized product) in GC analysis. However, it is well known that oligomerization of glycerol takes place at high temperature in the presence of strong acid catalyst [11]. On the other hand, formation of DGTA is significant when the concentration of DAG is high (e.g. after 4 h), which indicates that DGTA is the oligomer of DAG (see Fig. 5). Formation of DGTA was confirmed by GC-MS using authentic compound. Interestingly, except DGTA any other by-product (e.g. dehydrated product acrolein) was not observed.

### 3.4. Reusability, stability and homogeneous catalyst tests

Reusability and stability of the catalysts STA/SiO<sub>2</sub> and TPA/SiO<sub>2</sub> was tested by filtering off the catalyst after 10 h of reaction time and re-using it in another cycle under same reaction conditions (Fig. 7). The results from the 1st catalytic run with both the catalysts are very similar to the results obtained after 10 h in the runs described above (see Fig. 5), which proves that results are reproducible. In both runs, marginal decreases in glycerol conversion were observed for STA/SiO<sub>2</sub> (100% to 97%) and TPA/SiO<sub>2</sub> (100% to 94%), however, the high selectivity to TAG was not maintained dur-

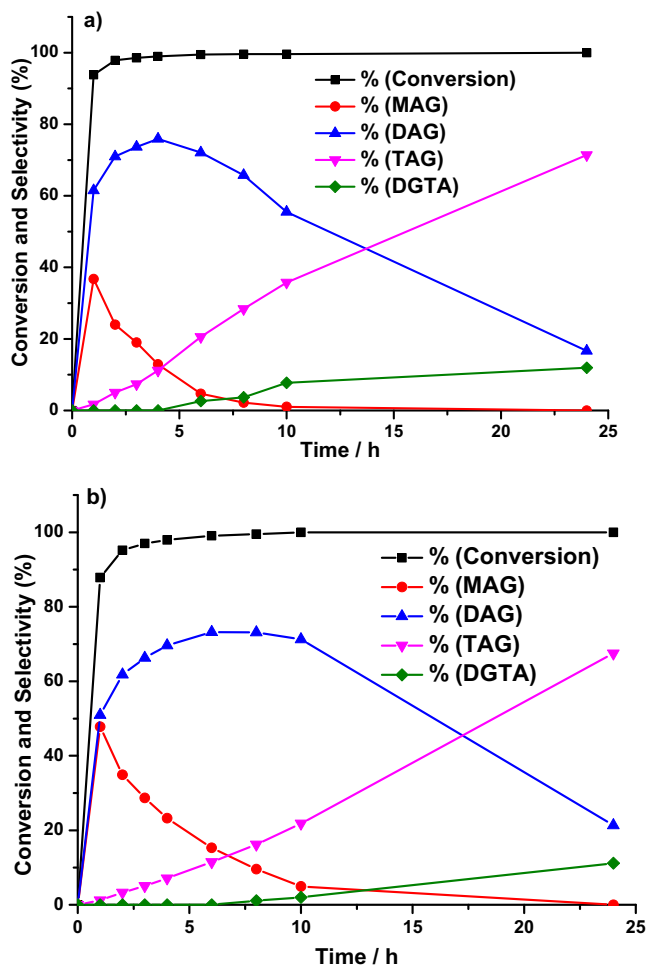


**Fig. 6.** Glycerol conversion and selectivities to products over a) STA/SiO<sub>2</sub> and b) TPA/SiO<sub>2</sub> during 24 h reaction (glycerol = 10 g, acetic acid = 39.16 g, molar ratio acetic acid: glycerol = 6: 1, toluene = 60 g, catalyst = 0.5 g, 105 °C).

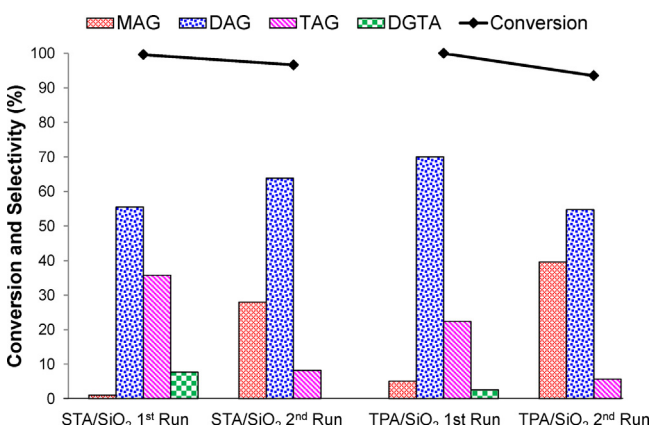


**Fig. 7.** Reusability results on glycerol acetylation in the presence of toluene as an entrainer over STA/SiO<sub>2</sub> and TPA/SiO<sub>2</sub> (glycerol = 10 g, acetic acid = 39.16 g, molar ratio acetic acid: glycerol = 6: 1, toluene = 60 g, catalyst = 0.5 g, 105 °C, time = 10 h).

**Table 4**  
ICP-OES analysis of the fresh and spent catalysts STA/SiO<sub>2</sub> and TPA/SiO<sub>2</sub>.

Catalyst	Element load, wt%	
	W	P
STA/SiO <sub>2</sub> <sup>a</sup>	Fresh	14.7
	Spent	8.2
TPA/SiO <sub>2</sub>	Fresh	14.4
	Spent	10.4

<sup>a</sup> Due to the silica support used, amount of leaching of Si from STA was not estimated.

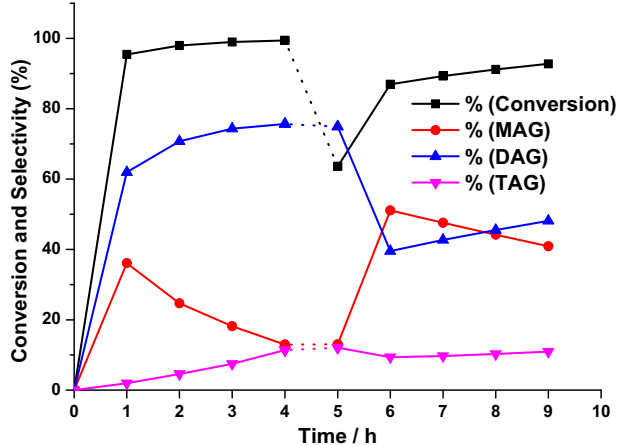


**Fig. 8.** Glycerol conversion and selectivities with 0.5 g of STA/SiO<sub>2</sub> in stop-experiment (reaction condition same as Fig. 6). The dotted lines represent the time period for catalyst removal and addition of fresh feed.

ing the recycle for both the catalysts. There was a considerable drop in TAG selectivity with STA/SiO<sub>2</sub> (35.8% to 8%) and TPA/SiO<sub>2</sub> (22.4% to 5.7%), indicating a lower overall turnover number in esterification. Thus, the selectivity toward TAG serves as a measure for the catalyst performance rather than the initial glycerol conversion. It is important to note that, formation of DGTA was not observed in the reusable test with both catalysts. In addition, the turnover number (TON) for all the products obtained over these two catalysts was calculated considering Bronsted acid sites and representing an individual esterification step. After 1<sup>st</sup> catalytic run with STA/SiO<sub>2</sub>, TON for MAG, DAG, TAG and DGTA were 8, 437, 281 and 60 and after recycle test TON changed to 65, 502, 220 and 0, respectively. Similar for TPA/SiO<sub>2</sub> after 1<sup>st</sup> catalytic run, TON for MAG, DAG, TAG and DGTA were 70, 982, 314 and 35 and after recycle test 555, 767, 79 and 0.

**Table 4** summarizes the results from ICP analyses of fresh and spent catalysts after 2<sup>nd</sup> run (STA/SiO<sub>2</sub> and TPA/SiO<sub>2</sub>) and illustrates the quantity of active component (tungsten) being leached into the reaction mixture leading to a decrease in the catalytic activity. The tungsten content of the catalysts decreased from 14.7% to 8.2% and 14.4% to 10.4%, respectively.

In order to clarify whether the leached part still contributes to glycerol acetylation via homogeneous catalysis, a separate stop experiment was performed with best performing catalyst STA/SiO<sub>2</sub> under identical conditions as depicted in Fig. 8. The catalyst was filtered off from the reaction mixture after 4 h when the selectivities for MAG, DAG and TAG were 12.9%, 75.7% and 11.4%, respectively, at almost complete conversion of glycerol.

After replenishing the consumed reactants (19.56 g of acetic acid, 5 g of glycerol, molar ratio = 6), the reaction was continued for another 4 h under the same conditions (except a slight increase in liquid volume) but in absence of the solid catalyst. The conversion of glycerol over the same time period of 4 h was slightly lower in

the second stage as well as the selectivity to DAG. The selectivity to MAG was somehow higher but selectivity to TAG did not increase further. Interestingly, the resulting conversion and selectivities (for MAG and DAG) were very similar to those of the blank test (cf. Table 3) showing a continuously increasing glycerol conversion; the initial very high selectivity to MAG decreased with time, the consecutive product DAG appears and TAG formation was never seen. May be leached species were disintegrated products of the active STA supported on silica, but did not longer exist as a Keggin anion structure. Literature reports on the interaction of a silica surface (silanols) and deposited TPA give some proofs on the formation of such surface anions [49]. Moreover, liquid phase reactions in acidic media lead to further decay to lacunary species [50]. However, the species formed by interaction of intact STA with silanols and the leached species were not able to catalyze the acetylation reaction efficiently (in contrast to the corresponding intact bulk HPA). Therefore, most likely the leached active species do not act as homogeneous catalyst. This means that the glycerol acetylation under given condition seems to be running on solid catalyst surfaces, i.e. intact HPA structure. It still has to be clarified whether the catalyst deactivation is due to simple loss of active species or if other effects like deposition of high-molecular oligomers (possibly formed in a similar way as DGTA) play a role.

#### 4. Conclusions

The combination of various HPAs and common support materials led only to few supported catalysts with remarkable performance that were able to produce triacetin (TAG) at high yield (71%) within acceptable time periods (24 h). Such catalysts were exclusively composed of tungsten-containing HPAs supported on silica. To achieve good performance, high Brønsted acidity is required, which seems to be linked first of all to the preservation of the Keggin structure of the HPAs with its high number of reactive protons. Other prerequisites to get effective catalysts of this type are the thermal stability of HPAs and a tuned strength of their interaction with the support. This is ensured if supports like silica without any Brønsted and Lewis sites are used and the deposited amount of HPA is rather high, otherwise, surface reactions of silanol groups with Keggin units lead to undesired surface species. Beyond that, it seems to be detrimental to use supports that possess remarkable intrinsic acidity, independent whether this is of Brønsted or Lewis type. This is typical for the alumina containing supports in this study. In such case, the acid sites of HPA and support may react with each other partially during the calcination at elevated temperature.

Some of these features of the fresh catalysts (low bonding strength between intact heteropolyacid crystallites and supports and/or disintegration of Keggin units due to surface reactions with silanol groups) in combination with the high polarity and hydrophilicity of unreacted glycerol and acetic acid are most likely responsible for the partial leaching of active component into the liquid phase and catalyst deactivation. Surprisingly, such leachate does not much contribute to catalytic activity in esterification. This might be due to the use of the entrainer toluene to establish water-free conditions, which suppresses the formation of Brønsted acids away from the solid supported catalysts. The use of an entrainer is definitely beneficial for the overall process as the chemical equilibrium of the esterification is shifted toward the target product triacetin. To make the catalysts more stable, a proper balance has to be found between the described intra- and intercrystallite interactions to preserve the HPAs structure and simultaneously to strengthen the bonding to the support to avoid leaching. A principal drawback of the applied reaction system is the missing option to adjust the reaction temperature; this is solely controlled by

boiling point of the reaction mixture, which itself changes during the progress of the reaction. To overcome this limitation for further optimization, a simultaneous control of reaction pressure would be necessary.

#### Acknowledgements

The authors would like to thank Mrs. A. Simmula for ICP analyses. The authors gratefully acknowledge the financial support by Deutsches Zentrum für Luft- und Raumfahrt e.V. (DLR, Germany) within the frame of the Bundesministerium für Bildung und Forschung (BMBF, Germany) – Council for Scientific and Industrial Research (CSIR, India) Cooperative Science Program (project number IND 11/045).

#### References

- [1] OECD/FAO (2011), OECD-FAO Agricultural Outlook 2011–2020, OECD Publishing and FAO. [http://dx.doi.org/10.1787/agr\\_outlook-2011-en](http://dx.doi.org/10.1787/agr_outlook-2011-en) pp. 77–93.
- [2] B. Katryniok, S. Paul, F. Dumeignil, *ACS Catal.* 3 (2013) 1819–1834.
- [3] S. Bagheri, N.M. Julkapli, W.A. Yehye, *Renewable Sustainable Energy Rev.* 41 (2015) 113–127.
- [4] S. Sato, D. Sakai, F. Sato, Y. Yamada, *Chem. Lett.* 41 (2012) 965–966.
- [5] H. Atia, U. Armbruster, A. Martin, *J. Catal.* 258 (2008) 71–82.
- [6] H. Atia, U. Armbruster, A. Martin, *Appl. Cat. A Gen.* 393 (2011) 331–339.
- [7] A. Martin, U. Armbruster, H. Atia, *Eur. J. Lipid Sci. Technol.* 114 (2012) 10–23.
- [8] I. Gandarias, J. Requies, P.L. Arias, U. Armbruster, A. Martin, *J. Catal.* 290 (2012) 79–89.
- [9] N. Ozbay, N. Oktar, G. Dogu, T. Dogu, *Top. Catal.* 56 (2013) 1790–1803.
- [10] N. Viswanadham, S.K. Saxena, *Fuel* 103 (2013) 980–986.
- [11] A. Martin, M. Richter, *Eur. J. Lipid Sci. Technol.* 113 (2011) 100–117.
- [12] C.H. Zhou, J.N. Beltramini, Y.X. Fan, G.Q. Lu, *Chem. Soc. Rev.* 37 (2008) 527–549.
- [13] M. Popova, A. Szegedi, A. Ristic, N.N. Tusar, *Catal. Sci. Technol.* 4 (2014) 3993–4000.
- [14] I. Kim, J. Kim, D. Lee, *Appl. Cat. B Environ.* 148–149 (2014) 295–303.
- [15] N. Rahmat, A.Z. Abdullah, A.R. Mohamed, *Renewable Sustainable Energy Rev.* 14 (2010) 987–1000.
- [16] X. Liao, Y. Zhu, S.G. Wang, H. Chen, Y. Li, *Appl. Catal. B* 94 (2010) 64–70.
- [17] M.L. Testa, V.L. Parola, L.F. Liotta, A.M. Venezia, *J. Mol. Catal. A: Chem.* 367 (2013) 69–76.
- [18] J.A. Malero, R.V. Grieken, G. Morales, M. Paniagua, *Energy Fuels* 21 (2007) 1782–1791.
- [19] I.D. Rodriguez, C. Adriany, E.M. Gaigneaux, *Catal. Today* 167 (2011) 56–63.
- [20] P.S. Reddy, P. Sudarsanam, G. Raju, B.M. Reddy, *J. Ind. Eng. Chem.* 18 (2012) 648–654.
- [21] M.S. Khayoon, B.H. Hameed, *Bioresour. Technol.* 102 (2011) 9229–9235.
- [22] T.S. Galhardo, N. Simone, M. Goncalves, F.C.A. Figueiredo, D. Mandelli, W.A. Carvalho, *ACS Sustainable Chem. Eng.* 1 (2013) 1381–1389.
- [23] L. Li, S.T. Yu, C.X. Xie, F.S. Liu, H.J. Li, *J. Chem. Technol. Biotechnol.* 84 (2009) 1649–1652.
- [24] I.D. Rodriguez, E.M. Gaigneaux, *Catal. Today* 195 (2012) 14–21.
- [25] L. Zhou, E. Al-Zaini, A.A. Adesina, *Fuel* 103 (2013) 617–625.
- [26] L. Zhou, E. Al-Zaini, A.A. Adesina, *Fuel Process. Technol.* 104 (2012) 310–318.
- [27] X. Liao, Y. Zhu, S.G. Wang, Y. Li, *Fuel Process. Technol.* 90 (2009) 988–993.
- [28] L.N. Silva, L.C. Valter, C.J.A. Mota, *Catal. Commun.* 11 (2011) 1036–1039.
- [29] P. Ferreira, I.M. Fonseca, A.M. Ramos, J. Vital, J.E. Castanheiro, *Catal. Commun.* 10 (2009) 481–484.
- [30] A. Patel, S. Singh, *Fuel* 118 (2014) 358–364.
- [31] S. Singh, A. Patel, *Ind. Res. Chem. Res.* 53 (2014) 14592–14600.
- [32] S. Zhu, Y. Zhu, X. Gao, T. Mo, Y. Zhu, Y. Li, *Biores. Technol.* 130 (2013) 45–51.
- [33] M. Huang, X. Han, C. Hung, J. Lin, P. Wu, J. Wu, S. Liu, J. Catal. 320 (2014) 42–51.
- [34] S. Kale, S.B. Umbarkar, M.K. Dongare, R. Eckelt, U. Armbruster, A. Martin, *Appl. Catal. A* 490 (2015) 10–16.
- [35] G. Mestl, T. Ilkenhans, D. Spielbauer, M. Dieterle, O. Timpe, J. Kröhnert, F.C. Jentoft, H. Knözinger, R. Schlögl, *Appl. Catal. A* 210 (2001) 13–34.
- [36] N. Legagneux, J.M. Basset, A. Thomas, F. Lefebvre, A. Gojet, J. Sa, C. Haedacre, *Dalton Trans.* 12 (2009) 2235–2240.
- [37] S. Damyanov, J.L.G. Fierro, *Chem. Mater.* 10 (1998) 871–879.
- [38] T.M. McEvoy, K.J. Stevenson, *Langmuir* 21 (2005) 3521–3528.
- [39] S.-X. Guo, A.W.A. Mariotti, C. Schlipf, A.M. Bond, A.G. Wedd, *Inorg. Chem.* 45 (2006) 8563–8574.
- [40] T.H. Kang, J.H. Choi, Y. Bang, J. Yoo, J.H. Song, W. Joe, J.S. Choi, I.K. Song, *J. Mol. Catal. A: Chem.* 396 (2015) 282–289.
- [41] G. Busca, *PCCP* 1 (1999) 723–736.
- [42] R. Buzzoni, S. Bordiga, G. Ricciardi, C. Lamberti, A. Zecchina, *Langmuir* 12 (1996) 930–940.
- [43] C.A. Emeis, *J. Catal.* 141 (1993) 347–354.
- [44] A.G. Alejandre, P. Castillo, J. Ramírez, G. Ramis, G. Busca, *Appl. Catal. A* 216 (2001) 181–194.

- [45] S.V. Gadekar, R.V. Naik, S.N. Kaul, J. Sci. Ind. Res. 68 (2009) 871–875.
- [46] I.V. Kozhevnikov, Chem. Rev. 98 (1988) 171–198.
- [47] S. Sato, K. Sagara, H. Furuta, F. Nazaki, J. Mol. Catal. A: Chem. 114 (1996) 209–216.
- [48] B.B. Bardin, S.V. Bordawekar, M. Neurock, R.J. Davis, J. Phys.Chem. B 102 (1998) 10817–10825.
- [49] J. Haber, K. Pamin, L. Matachowski, B. Napruszewska, J. Połtowicz, J. Catal. 207 (2002) 296–306.
- [50] L.R. Pizzio, C.V. Cáceres, M.N. Blanco, Appl. Catal. A 167 (1998) 283–294.